Figure 1 | Rupture map and offset measurements. a, 1931 rupture trace (red), mapped from Quickbird satellite image swath (swath limits indicated by thin lines). **b**, 569 horizontal offset measurements along the south-central part of the rupture from retrofitting of geomorphic markers into initial alignment. Error bars depend on the quality of measurements (see text and Supplementary Material for discussion). **c**, Horizontal offset distribution. Note the number of measurements decreasing exponentially with increasing offset size.

40 km of rupture, where normal faulting is dominant, is not included in this average. Based on this average value, scaling laws linking magnitude, average-slip and rupture-length for strike-slip earthquakes[23] yield $M_w = 7.6$, consistent with the magnitude M_s (7.9) derived from seismological data[24]. The slip distribution obtained (Fig. 1) shows no prominent displacement peak, even though one might be possible in the field near Karaxingar[22] (Supplementary Fig. S3 and Table S2). Sections with smaller than average coseismic slip, often marking segment boundaries[21,25], are not observed either. We cannot exclude the possibility that either minimum or maximum values might be located in some of the Quickbird data gaps, but outside such gaps the 1931 earthquake slip function does look unusually uniform, unlike those of several other earthquakes of similar magnitude, which show more variability along strike[21,25–27].

We interpret the second data subset of 279 larger offsets as representing the cumulative effect of several earthquakes, including the 1931 event. The implicit assumption—that the climatic modification of landforms occurs faster than earthquake disruption—seems justified by the slow slip-rate[28] and the millennial return time of great events[29] in a temperate continental climatic environment at latitude 46–47 N. The statistical distribution of cumulative offsets shows at least three well-defined and well-separated peaks, and more in places (Fig. 1). Such peaks are best documented along the northern and, most remarkably, central segment, where up to five regularly spaced clusters of values are clear. Using a discrete Fourier transform (Supplementary Method, Figs S4 and S5), we determine the characteristic wavelength Λ of the distribution to be 6.24 m, on par with the average slip l_c of the 1931 event. This indicates that, within error, the successive peaks at 12, 18, 24, 30 and possibly even 37 m in the offset distribution (Fig. 1) may represent the added displacements of 2, 3, 4, 5 and perhaps 6 great earthquakes, each with a very similar slip, implying that up to half a dozen successive event ruptures along the Fuyun fault followed a characteristic slip pattern. Although the occurrence of smaller magnitude events, associated with smaller offsets, cannot be completely ruled out, we found no convincing evidence of any.

To test quantitatively how many characteristic slip events each of the 279 displacement values might represent, we model a theoretical distribution of offsets based on the 1931 slip function and the assumption of characteristic coseismic slip. To account for the fact that the number of observations decreases exponentially with increasing offset (Fig. 1), that is, with the number of events and hence with time, we introduce a constant (λ, characterizing the rate of preservation of geomorphic markers) that integrates all degradation factors, natural or anthropological (see Supplementary Method). This constant averages local conditions over the 110 km studied and can be used on a regional basis to quantify the ageing of landforms as a function of time. In a way, it characterizes the resilience of geomorphic memory. Here, along the eastern edge of the Jungar basin, the constant that best fits the dataset in Fig. 1 is $\lambda = 0.55$. Figure 3 shows the results of the modelling in the form of a probability density function (PDF) superimposed on the original dataset, with data points coded by symbols indicating the number of events. The number of events attributed to each measured cumulative offset reflects the highest calculated probability density (see Supplementary Method). The penultimate event is well defined along most of the length of the fault studied, with cumulative offsets twice as large as the smallest offsets associated with the 1931 earthquake. The third event back in time is also well defined between 5 and 75 km. Despite sparser data, the fit between measured offset and predicted event number remains satisfactory for the fourth and fifth events, especially between 47 and 65 km. The larger offset values around 37 m, although fewer than ten in number, hint at the possible record of a sixth earthquake. The simple pattern of clear first multiples observed between 5 and 80 km, however, breaks

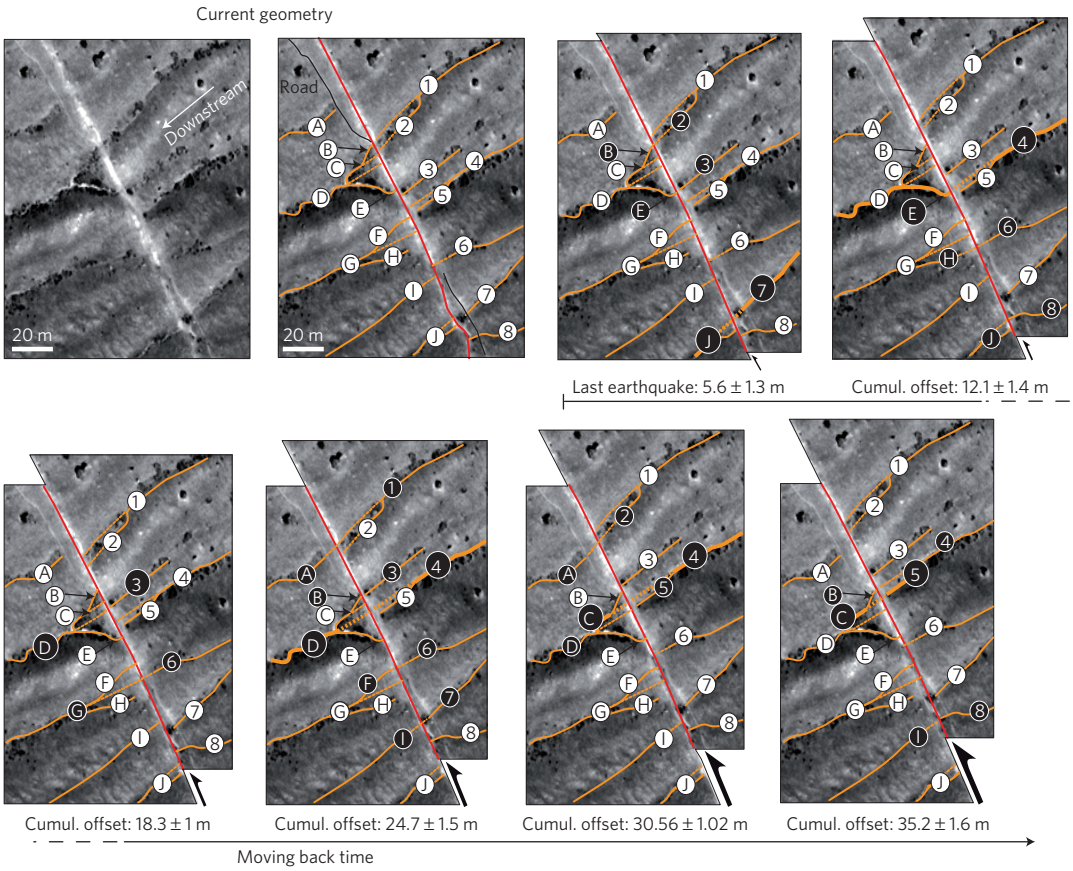

Figure 2 | Successive reconstructions of offset channels at site 4D (location on Fig. 1). Channels are labelled alphabetically and numerically on the west and east sides of fault, respectively. Starting from the present geometry, the east side is moved to realign channels truncated or disconnected as the result of successive earthquakes. Each offset is determined by restoring continuity of one main channel (large black circle) and other secondary channels (small black circles). Successive offsets of 5.6, 12.1, 18.3, 24.7, 30.56 and 35.2 m are identified.

down at the southern end of the rupture. This is also where the two independent field surveys[17,22] depart most significantly from one another. This may be taken to indicate the existence of additional offsets resulting from an earthquake other than the 1931 event, for which the rupture might have propagated northwards from the southernmost stretch of the fault south of Ertai.

Overall, our 'Quickbird' dataset indicates that local coseismic slip for successive earthquakes on the central 80 km of the Fuyun fault was very similar, pointing to a characteristic slip behaviour[1]. The successive ruptures seem to have propagated across step-overs as wide as 2.2 km, as observed elsewhere[10]. As no direct dating is available for the cumulative offsets, the ages of earthquakes predating 1931 are unknown. Hence, it remains possible that such earthquakes ruptured only part of the stretch of the fault that slipped during the last event. However, the facts that the two main segment boundaries are not strongly expressed geomorphically and that neither is well marked in the 1931 slip distribution make this unlikely. Moreover, any such earthquake would have had an unduly large slip relative to rupture length, an observation clearly at odds with general scaling laws. This does suggest that the last five earthquakes on the fault were close to characteristic, a rather unexpected circumstance along strike-slip faults[1], but not altogether implausible here. Indeed, in this northernmost boundary zone of the India/Asia collision zone, the present deformation is fairly complex and slow. It is absorbed by several rather short fault systems which slip at only a few mm yr^{-1} (refs 28,30) and have finite offsets of at most a few tens of km (~25 km for the Fuyun fault, Fig. 1). It is thus likely that even strike-slip faults here are in an immature stage of development and still growing. Clearly,

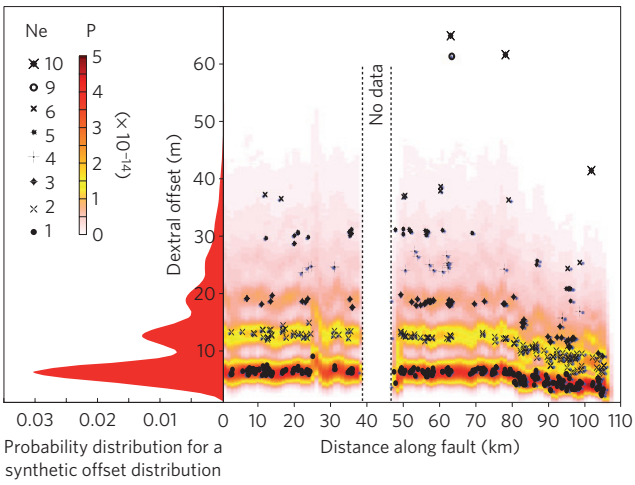

Figure 3 | Direct slip distribution modelling. Comparison between measurements and synthetic density probabilities (P) computed from 1931 initial slip distribution, assuming characteristic slip and exponential decay of landforms. Offset values are coded with symbols representing the most probable number of earthquakes (Ne) required to create them.

dating the occurrence of past earthquakes on the different segments of the fault is the only way to resolve this issue, and determine whether the Fuyun fault still behaves in a characteristic-earthquake mode or if individual segments rupture independently and link opportunistically, producing earthquakes with a more diverse range

of magnitudes and occurrence times, as is usually the case along strike-slip plate boundaries.

Received 25 February 2011; accepted 19 April 2011; published online 22 May 2011

References

1. Sieh, K. The repetition of large-earthquake ruptures. *Proc. Natl Acad. Sci. USA* **93,** 3764–3771 (1996).
2. Shimazaki, K. & Nakata, T. Time-predictable recurrence model for large earthquakes. *Geophys. Res. Lett.* **7,** 279–282 (1980).
3. Bakun, W. & McEvilly, T. V. Recurrence models and Parkfield, California. *J. Geophys. Res.* **89,** 3051–3058 (1984).
4. Weldon, R., Fumal, T. & Biasi, G. P. Wrightwood and the earthquake cycle: What a long recurrence record tells us about how faults work. *GSA Today* **14,** 4–10 (2004).
5. Sieh, K. Lateral offsets and revised dates of large earthquakes at Pallett Creek, California. *J. Geophys. Res.* **89,** 7641–7670 (1984).
6. Daëron, M. *et al.* 12,000-year-long record of up to 14 paleo-earthquakes on the Yammoûneh fault (Levant fault system). *Bull. Seismol. Soc. Am.* **97,** 749–771 (2007).
7. Klinger, Y. *et al.* Paleoseismic evidence of characteristic slip on the western segment of the North Anatolian Fault, Turkey. *Bull. Seismol. Soc. Am.* **93,** 2317–2332 (2003).
8. Liu, J., Klinger, Y., Sieh, K. & Rubin, C. Six similar sequential ruptures of the San Andreas fault, Carrizo Plain, California. *Geology* **32,** 649–652 (2004).
9. Zielke, O., Arrowsmith, J. R., Grant Ludwig, L. & Akçiz, S. O. Slip in the 1857 and earlier large earthquakes along the Carrizo Plain, San Andreas fault. *Science* **327,** 1119–1122 (2010).
10. Wesnousky, S. Predicting the endpoints of earthquake ruptures. *Nature* **444,** 358–360 (2006).
11. Klinger, Y. Relation between continental strike-slip earthquake segmentation and thickness of the crust. *J. Geophys. Res.* **115,** B07306 (2010).
12. Lindvall, S., Rockwell, T. & Hudnut, K. Evidence for prehistoric earthquakes on the Superstition Hills fault from offset geomorphic features. *Bull. Seismol. Soc. Am.* **79,** 342–361 (1989).
13. Kondo, H. *et al.* Slip distribution, fault geometry, and fault segmentation of the 1944 Bolu-Gerede earthquake rupture, North Anatolian Fault, Turkey. *Bull. Seismol. Soc. Am.* **95,** 1234–1249 (2005).
14. Tapponnier, P. & Molnar, P. Active faulting and Cenozoic tectonics of the Tien Shan, Mongolia and Baykal regions. *J. Geophys. Res.* **84,** 3425–3459 (1979).
15. Ding, G. (ed.) *The Fuyun Earthquake Fault Zone in Xinjiang, China* (Seismol. Press, 1985).
16. Kanamori, H. in *Historical Seismograms and Earthquakes of the World* (eds Lee, W. H. K., Meyers, H. & Shimazaki, K.) (Academic, 1988).
17. Jianbang, S., Xianyue, S. & Shumo, G. *International Symposium on Continental Seismicity and Earthquake Prediction* (Seismol. Press, 1984).
18. Awata, Y., Fu, B. & Zhang, Z. Re-investigation of the geometry and slip distribution of the 1931 Fuyun surface rupture, northwest China. *AGU (Fall meeting Suppl.)* abstr. #no. T41A-1930 (2008).
19. Lienkaemper, J. 1857 slip on the San Andreas fault southeast of Cholame, California. *Bull. Seismol. Soc. Am.* **91,** 1659–1672 (2001).
20. Rockwell, T. *et al.* Lateral offsets on surveyed cultural features resulting from the 1999 Izmit and Duzce earthquakes, Turkey. *Bull. Seismol. Soc. Am.* **92,** 79–94 (2002).
21. Klinger, Y., Michel, R. & King, G. C. P. Evidence for an earthquake barrier model from Mw similar to 7.8 Kokoxili (Tibet) earthquake slip-distribution. *Earth Planet. Sci. Lett.* **242,** 354–364 (2006).
22. Lin, A. & Lin, S. Tree damage and surface displacement: The 1931 M 8.0 Fuyun earthquake. *J. Geol.* **106,** 751–757 (1998).
23. Wells, D. L. & Coppersmith, K. J. New empirical relationships among magnitude, rupture length, rupture width, rupture area, and surface displacement. *Bull. Seismol. Soc. Am.* **84,** 974–1002 (1994).
24. Lee, W. H. K., Kanamori, H., Jennings, P. C. & Kisslinger, C. *International Handbook of Earthquake and Engineering Seismology* (Academic, 2002).
25. Sieh, K. *et al.* Near-Field investigations of the Landers earthquake sequence, April to July 1992. *Science* **260,** 171–176 (1993).
26. Haeussler, P. J. *et al.* Surface rupture and slip distribution of the Denali and Totschunda faults in the 3 November 2002 M 7.9 earthquake, Alaska. *Bull. Seismol. Soc. Am.* **94,** S23–S52 (2004).
27. Wesnousky, S. G. Displacement and geometrical characteristics of earthquake surface ruptures: Issues and implications for seismic-hazard analysis and the process of earthquake rupture. *Bull. Seismol. Soc. Am.* **98,** 1609–1632 (2008).
28. Calais, E. *et al.* GPS measurements of crustal deformation in the Baikal–Mongolia area (1994–2002): Implications for current kinematics of Asia. *J. Geophys. Res.* **108,** 2501 (2003).
29. Shumo, G., Meixiang, B., Daozun, X. & Zhiyong, X. The recurrence intervals of major earthquakes at the active koktokay-Ertai fault. *Earthq. Res. China* **2,** 67–80 (1986).
30. Baljinnyam, I. *et al. Ruptures of Major Earthquakes and Active Deformation in Mongolia and its Surroundings, Geological Society of America Memoir 181* (The Geological Society of America, 1993).

Acknowledgements

Thanks are extended to the CNES, which gave us access to imagery in the framework of the Pleiade preparation program. We thank R. Arrowsmith and G. Biasi for constructive reviews. This is IPGP contribution 3157, and EOS contribution 20.

Author contributions

M. E. carefully mapped offset markers along the fault. C.N. took care of much of the statistical modelling effort. They, and all other authors, equally participated in the completion of the work.

Additional information

The authors declare no competing financial interests. Supplementary information accompanies this paper on www.nature.com/naturegeoscience. Reprints and permissions information is available online at http://www.nature.com/reprints. Correspondence and requests for materials should be addressed to Y.K.